

# Nuclear spin-lattice relaxation rate in noncentrosymmetric superconductor $Y_2C_3$

Chongju Chen<sup>a</sup>, Biao Jin<sup>a,\*</sup>

<sup>a</sup>*School of Physical Sciences, University of Chinese Academy of Sciences - BeiJing 100049  
China*

---

## Abstract

For a noncentrosymmetric superconductor such as  $Y_2C_3$ , we consider a parity-mixing model composed of spin-singlet  $s$ -wave and spin-triplet  $f$ -wave pairing components. The  $d$ -vector in  $f$ -wave state is chosen to be parallel to the Dresselhaus asymmetric spin-orbit coupling vector. It is found that, the quasiparticle excitation spectrum exhibits distinct nodal structure as a consequence of parity-mixing. Our calculation predict anomalous noninteger power laws for low-temperature nuclear spin-lattice relaxation rate  $T_1^{-1}$ . We demonstrate particularly that such a model can qualitatively account for the existing experimental results of the temperature dependence of  $T_1^{-1}$  in  $Y_2C_3$ .

*Keywords:* Noncentrosymmetric superconductor  $Y_2C_3$ , Pairing symmetry, Nuclear spin-lattice relaxation rate  
*PACS:* 74.20.Rp, 74.20.-z, 74.25.Bt

---

## 1. Introduction

The physics of unconventional superconductivity in materials without inversion symmetry has become a subject of growing interest [1, 2] since the noncentrosymmetric (NCS) heavy Fermion superconductor  $CePt_3Si$  was found in 2004 [3]. In these materials the superconducting phase develops in a low-symmetry environment with a missing inversion center. This broken symmetry generates

---

\*Corresponding author  
*Email address:* biaojin@ucas.ac.cn (Biao Jin)

an antisymmetric spin-orbit (SO) coupling and prevent the usual even/odd classification of Cooper pairs according to orbital parity, allowing a mixed-parity superconducting state [4, 5]. This mixture of the pairing channels with different parities may result in unusual temperature and field dependence of experimentally observed superconducting properties [1, 2].

For CePt<sub>3</sub>Si, in particular, where the Rashba-type [6] SO coupling vector  $\boldsymbol{\gamma}_{\mathbf{k}} \propto (\hat{k}_y, -\hat{k}_x, 0)$  is generated, various low-energy thermodynamical and transport properties have been extensively investigated from both the experimental and theoretical sides. The NMR relaxation rate [7]  $T_1^{-1}$ , thermal conductivity [8], and London penetration depth [9] indicate power law behavior at lowest temperatures, suggesting the presence of nodal lines in the quasiparticle excitation spectrum. Besides, the upper critical magnetic field  $H_{c2}$  is surprisingly large [3, 10], and no change in the Knight shift across the transition temperature  $T_c$  [11] has been observed. These characteristics are attributed to a spin triplet superconducting order parameter. Theoretically, Frigeri *et al.* have proposed an  $(s+p)$ -wave model [12] where the  $d$ -vector of  $p$ -wave state is chosen to be parallel to the SO coupling vector ( $\mathbf{d}_{\mathbf{k}} \propto \mathbf{g}_{\mathbf{k}}$ ). The gap function of this  $(s+p)$ -wave model has the natural form for a system without inversion symmetry, and exhibits line nodes when the  $p$ -wave pair potential is larger than that of  $s$ -wave one. It should be noted that a nonzero  $s$ -wave pair potential is necessary to get expected line nodes. Hayashi *et al.* [13] have demonstrated that the presence of line nodes in this  $(s+p)$ -wave model may account for the experimentally observed low-temperature features of the nuclear spin-lattice relaxation rate  $T_1^{-1}$  in CePt<sub>3</sub>Si on a qualitative level.

The cubic Pu<sub>2</sub>C<sub>3</sub>-type sesquicarbide compound Y<sub>2</sub>C<sub>3</sub> is a NCS superconductor known for its relatively high superconducting transition temperature [14] ( $T_c \sim 18\text{K}$ ). Different from the CePt<sub>3</sub>Si case, the Dresselhaus [15] SO coupling vector  $\boldsymbol{\gamma}_{\mathbf{k}} \propto (\hat{k}_x(\hat{k}_y^2 - \hat{k}_z^2), \hat{k}_y(\hat{k}_z^2 - \hat{k}_x^2), \hat{k}_z(\hat{k}_x^2 - \hat{k}_y^2))$  is relevant to Y<sub>2</sub>C<sub>3</sub>.

Even many years after its discovery, the nature and symmetry of the superconducting gap function in Y<sub>2</sub>C<sub>3</sub> appears to be full of contradiction. While the specific heat measurement [16] and tunneling experiment [17] are interpreted as

a fully gapped isotropic  $s$ -wave state, the nuclear spin-lattice relaxation rate [18]  $T_1^{-1}$  and muon spin rotation [19] ( $\mu$ SR) measurements on  $Y_2C_3$  are qualitatively fitted with a nodeless two-gap model similar to  $MgB_2$ . On the other hand, Chen *et al.* [20] have measured the magnetic penetration depth as a function of temperature and found a weak linear dependence at very low temperatures. They also reanalysed the NMR data reported in Ref. [18] and claimed that, where  $T_1^{-1} \sim T^3$  at  $T < 3K$ , as a matter of fact. Such behavior seems to support the existence of line nodes rather than a fully opened gap in the superconducting state of  $Y_2C_3$ . In addition, the upper critical magnetic field  $H_{c2}$  is found to be compatible with the paramagnetic limiting field [10, 20], and the Knight shift in NMR [18] is decreased to approximately 2/3 of its normal-state value. These features are again incompatible with the single gap or two-gap  $s$ -wave pictures. It is expected that line nodes (or point nodes of second-order) would be generated due to parity-mixing, similar to the case of  $CePt_3Si$  mentioned above. In order to shed light on these controversy, further experimental and theoretical studies on the superconducting properties of  $Y_2C_3$  are required.

In this work, we theoretically investigate the nuclear spin-lattice relaxation rate [18]  $T_1^{-1}$  on the basis of  $(s+f)$ -wave model, where the  $d$ -vector in  $f$ -wave state is chosen to be parallel to the Dresselhaus-type asymmetric SO coupling vector. We analyse various possible nodal structures which can be generated by the effect of parity-mixing. In particular, the temperature dependence of the nuclear spin-lattice relaxation rate  $T_1^{-1}$  is calculated and compared with the experimental result obtained in Ref. [18] for  $Y_2C_3$ .

## 2. Model Hamiltonian

Our starting point is the following mean-field  $(s+f)$ -wave pairing Hamiltonian

$$H = H_0 + H_{int}. \quad (1)$$

The Hamiltonian  $H_0$  describes the noninteracting conduction electrons in a NCS crystal,

$$H_0 = \sum_{\mathbf{k}} \sum_{\alpha, \beta} (\epsilon_{\mathbf{k}} \sigma_0 + \gamma_0 \boldsymbol{\gamma}_{\mathbf{k}} \cdot \boldsymbol{\sigma})_{\alpha\beta} c_{\mathbf{k}\alpha}^\dagger c_{\mathbf{k}\beta}, \quad (2)$$

where  $c_{\mathbf{k}\alpha}^\dagger$  ( $c_{\mathbf{k}\alpha}$ ) creates (annihilates) an electron with wave vector  $\mathbf{k}$  and spin  $\alpha$ ,  $\boldsymbol{\sigma} = (\sigma_x, \sigma_y, \sigma_z)$  denotes the vector of Pauli matrices,  $\sigma_0$  is the  $2 \times 2$  unit matrix,  $\epsilon_{\mathbf{k}}$  is the parabolic bare band dispersion measured relative to the chemical potential restricted to  $|\epsilon_{\mathbf{k}}| < \omega_c$ , with  $\omega_c$  being the usual cutoff energy. Furthermore,  $\boldsymbol{\gamma}_{\mathbf{k}} = (\hat{k}_x(\hat{k}_z^2 - \hat{k}_y^2), \hat{k}_y(\hat{k}_z^2 - \hat{k}_x^2), \hat{k}_z(\hat{k}_x^2 - \hat{k}_y^2))$ , with  $\hat{k}_x = \sin \theta_{\mathbf{k}} \cos \phi_{\mathbf{k}}$ ,  $\hat{k}_y = \sin \theta_{\mathbf{k}} \sin \phi_{\mathbf{k}}$ , and  $\hat{k}_z = \cos \theta_{\mathbf{k}}$ , is the asymmetric ( $\boldsymbol{\gamma}_{\mathbf{k}} = -\boldsymbol{\gamma}_{-\mathbf{k}}$ ) Dresselhaus SO coupling vector considered to be relevant for  $\text{Y}_2\text{C}_3$  and  $\text{La}_2\text{C}_3$ . The strength of SO coupling is denoted by  $\gamma_0$ .

The second term in Eq. (1) represents the pairing interaction:

$$H_{int} = \frac{1}{2} \sum_{\mathbf{k}} \sum_{\alpha, \beta} [\Delta_{\mathbf{k}, \alpha\beta} c_{\mathbf{k}\alpha}^\dagger c_{-\mathbf{k}\beta}^\dagger + \Delta_{\mathbf{k}, \alpha\beta}^\dagger c_{-\mathbf{k}\alpha} c_{\mathbf{k}\beta} + \Delta_{\mathbf{k}, \alpha\beta} F_{\mathbf{k}, \beta\alpha}^\dagger],$$

with the anomalous averages  $F_{\mathbf{k}, \alpha\beta} = \langle c_{\mathbf{k}\alpha} c_{-\mathbf{k}\beta} \rangle$ , and the gap function defined by [21]

$$\Delta_{\mathbf{k}, \alpha\beta} = - \sum_{\mathbf{k}'} \sum_{\lambda, \mu} V_{\beta\alpha, \lambda\mu}(\mathbf{k}, \mathbf{k}') F_{\mathbf{k}', \lambda\mu}, \quad (3)$$

where  $V_{\alpha\beta, \lambda\mu}(\mathbf{k}, \mathbf{k}')$  is the pairing potential. In this work, we will adopt  $V_{\alpha\beta, \lambda\mu}(\mathbf{k}, \mathbf{k}')$  as the phenomenological one [22]:

$$V_{\alpha\beta, \lambda\mu}(\mathbf{k}, \mathbf{k}') = -\frac{V_s}{2} (i\sigma_y)_{\alpha\beta} (i\sigma_y)_{\lambda\mu}^\dagger - \frac{V_f}{2} (\boldsymbol{\gamma}_{\mathbf{k}} \cdot \boldsymbol{\sigma} i\sigma_y)_{\alpha\beta} (\boldsymbol{\gamma}_{\mathbf{k}'} \cdot \boldsymbol{\sigma} i\sigma_y)_{\lambda\mu}^\dagger + \frac{V_m}{2} [(\boldsymbol{\gamma}_{\mathbf{k}} \cdot \boldsymbol{\sigma} i\sigma_y)_{\alpha\beta} (i\sigma_y)_{\lambda\mu}^\dagger + (i\sigma_y)_{\alpha\beta} (\boldsymbol{\gamma}_{\mathbf{k}'} \cdot \boldsymbol{\sigma} i\sigma_y)_{\lambda\mu}^\dagger], \quad (4)$$

where the first two terms represent the interaction in the  $s$ -wave pairing channel and in the spin-triplet  $f$ -wave pairing channel, respectively, and the last term describes the scattering between the two channels. In the following, we will

chose the interaction parameters  $V_s$ ,  $V_f$ , and  $V_m$  to be positive, and take for simplicity  $V_m = \sqrt{V_s V_f}$  which yields  $\Delta_s(T)/\Delta_f(T) = \text{const.}$  [22].

Owing to the lack of inversion symmetry, the superconducting gap function Eq. (3) generally contains an admixture of even-parity spin-singlet and odd-parity spin-triplet pairing states,

$$\Delta_{\mathbf{k},\alpha\beta} = [\psi_{\mathbf{k}} i\sigma_y + \mathbf{d}_{\mathbf{k}} \cdot \boldsymbol{\sigma} i\sigma_y]_{\alpha\beta}, \quad (5)$$

where  $\psi_{\mathbf{k}} = \psi_{-\mathbf{k}}$  and  $\mathbf{d}_{\mathbf{k}} = -\mathbf{d}_{-\mathbf{k}}$  represent the spin-singlet and spin-triplet components, respectively. The direction of the  $\mathbf{d}_{\mathbf{k}}$  (the  $d$ -vector) is assumed to be parallel to  $\boldsymbol{\gamma}_{\mathbf{k}}$ , as for this choice the antisymmetric SO interaction is not destructive for spin-triplet pairing[12]. Hence, we parametrize the  $\mathbf{d}$ -vector as  $\mathbf{d}_{\mathbf{k}} = \Delta_f \boldsymbol{\gamma}_{\mathbf{k}}$ . For the spin-singlet component we assume  $s$ -wave pairing  $\psi_{\mathbf{k}} = \Delta_s$ , and choose the amplitudes  $\Delta_s$  and  $\Delta_f$  to be real and positive.

Using the vector operator  $\Psi_{\mathbf{k}} = (c_{\mathbf{k}\uparrow}, c_{\mathbf{k}\downarrow}, c_{-\mathbf{k}\uparrow}^\dagger, c_{-\mathbf{k}\downarrow}^\dagger)^t$ , where  $(\dots)^t$  stands for the transposing operation, we can write the Hamiltonian in a more compact form:

$$H = \frac{1}{2} \sum_{\mathbf{k}} \Psi_{\mathbf{k}}^\dagger \check{H}_{\mathbf{k}} \Psi_{\mathbf{k}} + \sum_{\mathbf{k}} \epsilon_{\mathbf{k}} + \frac{1}{2} \sum_{\mathbf{k}} \sum_{\alpha,\beta} \Delta_{\mathbf{k},\alpha\beta} F_{\mathbf{k},\beta\alpha}^\dagger, \quad (6)$$

where

$$\check{H}_{\mathbf{k}} = \begin{pmatrix} \hat{M}_{\mathbf{k}} & \hat{\Delta}_{\mathbf{k}} \\ \hat{\Delta}_{\mathbf{k}}^\dagger & -\hat{M}_{-\mathbf{k}}^* \end{pmatrix}, \quad (7)$$

with

$$\begin{aligned} \hat{M}_{\mathbf{k}} &= \epsilon_{\mathbf{k}} \sigma_0 + \gamma_0 \boldsymbol{\gamma}_{\mathbf{k}} \cdot \boldsymbol{\sigma}, \\ \hat{\Delta}_{\mathbf{k}} &= (\Delta_s + \Delta_f \boldsymbol{\gamma}_{\mathbf{k}} \cdot \boldsymbol{\sigma})(i\sigma_y). \end{aligned} \quad (8)$$

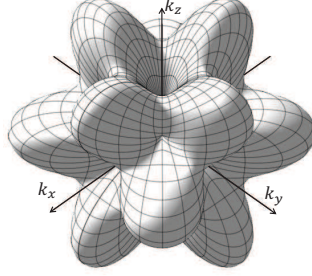


Figure 1: Schematic illustration of the amplitude of Dresselhaus SO coupling  $|\gamma_{\mathbf{k}}|$  in  $\mathbf{k}$  space.

### 3. Nodal structures

The Bogoliubov-de Gennes quasiparticle excitation spectrum  $E(\mathbf{k})$  can be obtained readily by diagonalizing the matrix  $\check{H}_{\mathbf{k}}$  above. One can find four solutions, namely,  $E_{\pm}^{(e)}(\mathbf{k})$  and  $E_{\pm}^{(h)}(\mathbf{k})$ , with  $E_{\pm}^{(h)}(\mathbf{k}) = -E_{\pm}^{(e)}(\mathbf{k})$ . We have

$$E_{\pm}^{(e)}(\mathbf{k}) = \sqrt{(\epsilon_{\mathbf{k}} \pm \gamma_0 |\gamma_{\mathbf{k}}|)^2 + (\Delta_s \pm \Delta_f |\gamma_{\mathbf{k}}|)^2} \equiv E_{\pm}^{\mathbf{k}}, \quad (9)$$

corresponding to two sheets of Fermi surfaces with the energy gaps given by  $\Delta_{\mathbf{k}+} = \Delta_s + \Delta_f |\gamma_{\mathbf{k}}|$  and  $\Delta_{\mathbf{k}-} = \Delta_s - \Delta_f |\gamma_{\mathbf{k}}|$ , respectively. Zeros of  $E_{\pm}^{\mathbf{k}}$  determine the nodal structure of the superconducting state in momentum space. Here let us assume a sufficiently large value of the cutoff energy  $\omega_c$  ( $\omega_c \gg \gamma_0, \Delta_s, \Delta_f$ ). It is apparent that the upper branch  $E_{+}^{\mathbf{k}}$  is positive definite. Therefore, here we focus on the zeros of the lower branch  $E_{-}^{\mathbf{k}}$ .

The amplitude of the Dresselhaus SO coupling  $|\gamma_{\mathbf{k}}|$  (see Fig. 1) becomes zero at 14 points (such as the south and north poles), possesses 24 saddle points at  $(\theta_{\mathbf{k}} = \arctan 2\sqrt{2}, \phi_{\mathbf{k}} = \arccos \sqrt{2}/4)$ , etc. with  $|\gamma_{\mathbf{k}}| = 2\sqrt{2}/9$ , and attains its maximum value 0.5 at 12 points  $(\theta_{\mathbf{k}} = \pi/2, \phi_{\mathbf{k}} = \pi/4)$ , etc. on the Fermi surface. Therefore, one encounters different nodal topology depending on the ratio  $\kappa \equiv \Delta_s/\Delta_f$ . When  $\kappa = 0$  ( $\kappa = 0.5$ ),  $E_{-}^{\mathbf{k}}$  shows 14 (12) nodal points of first-order (second-order), while exhibits line nodes for  $0 < \kappa < 0.5$  as displayed in Fig. 2. For  $\kappa > 0.5$ , however, we always have  $\Delta_{\mathbf{k}-} \neq 0$ , and thus the quasiparticle excitation spectrum is gapped.

#### 4. Nuclear magnetic relaxation rate

Let us consider the temperature dependence of the nuclear magnetic relaxation rate  $T_1^{-1}$  defined as

$$\frac{1}{T_1 T} \propto \sum_{\mathbf{q}} \frac{\Im[\chi_{-+}(\mathbf{q}, i\omega_n \rightarrow \omega + i0^+)]}{\omega} \Big|_{\omega \rightarrow 0}, \quad (10)$$

where  $\Im$  denotes the imaginary part. The dynamical susceptibility in imaginary time is given by

$$\chi_{-+}(\mathbf{q}, i\omega_n) = \int_0^{1/T} d\tau \sum_{\mathbf{k}\mathbf{k}'} \langle \hat{T} c_{\mathbf{k}'-\mathbf{q}\downarrow}^\dagger(\tau) c_{\mathbf{k}'\uparrow}(\tau) c_{\mathbf{k}+\mathbf{q}\uparrow}^\dagger(0) c_{\mathbf{k}\downarrow}(0) \rangle e^{i\omega_n \tau}, \quad (11)$$

where  $\hat{T}$  denotes the time-ordering operator,  $\omega_n = (2n+1)\pi T$  is the Matsubara frequency, and  $c_{\mathbf{k}}(\tau) = e^{iH\tau} c_{\mathbf{k}} e^{-iH\tau}$ . We obtain an explicit expression for  $T_1^{-1}$  as

$$\frac{1}{T_1 T} \propto \sum_{\mathbf{k}, \mathbf{q}} \sum_{\ell, j=\pm} \frac{\delta(E_\ell^{\mathbf{k}} - E_j^{\mathbf{q}})}{T \cosh^2(E_\ell^{\mathbf{k}}/2T)} \left( 1 + \frac{\epsilon_{\ell, \mathbf{k}} \epsilon_{j, \mathbf{q}} + \Delta_{\ell, \mathbf{k}} \Delta_{j, \mathbf{q}}}{E_\ell^{\mathbf{k}} E_j^{\mathbf{q}}} \right),$$

where  $\epsilon_{\pm, \mathbf{k}} = \epsilon_{\mathbf{k}} \pm \gamma_0 |\gamma_{\mathbf{k}}|$ . The temperature dependence of  $\Delta_s$  and  $\Delta_f$  are determined by the self-consistent gap equations:

$$\begin{aligned} \Delta_s &= \sum_{\mathbf{k}, \ell} \frac{\tanh(E_\ell^{\mathbf{k}}/2T)}{4E_\ell^{\mathbf{k}}} \Delta_{\ell, \mathbf{k}} (V_s + \ell V_m |\gamma_{\mathbf{k}}|), \\ \Delta_f &= \sum_{\mathbf{k}, \ell} \frac{\tanh(E_\ell^{\mathbf{k}}/2T)}{4E_\ell^{\mathbf{k}}} \Delta_{\ell, \mathbf{k}} (V_m + \ell V_f |\gamma_{\mathbf{k}}|). \end{aligned} \quad (12)$$

It turns out that for given values of  $V_s, V_f$ , and  $\omega_c$ ,  $1/T_1 T$  depends on the  $\Delta_s$  and  $\Delta_f$  only through the ratio  $\kappa$ , and is independent of the strength of SO coupling  $\gamma_0$ , similar to the case of Ref. [13]. It is interesting to see how the low-temperature power law behaviour for the nuclear spin-lattice relaxation rate  $1/T_1 T \propto T^n$  is changed with the ratio  $\kappa$ . Plotted in Fig. 3 is the exponent of temperature,  $n$ , as a function of  $\kappa$  at  $T = 0.04T_c$  calculated numerically according to  $n = d \ln(1/T_1 T) / d \ln T$  [23]. As we see, the exponent  $n$  attains its maximum  $n = 4$  at  $\kappa = 0$  (point node of first-order), decreases oscillatorily

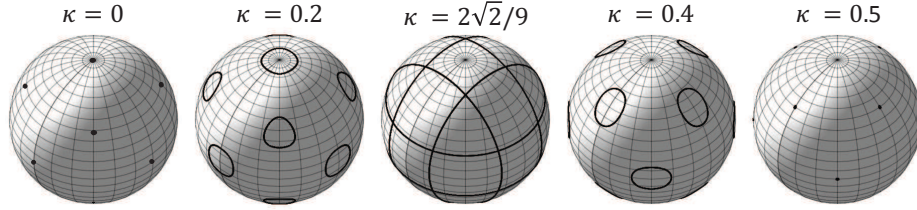


Figure 2: Evolution of nodal structure with the parameter  $\kappa$  ( $0 \leq \kappa \leq 0.5$ ). At  $\kappa = 0$  ( $\kappa = 0.5$ ),  $E_{\pm}^k$  shows 14 (12) nodal points of first-order (second-order), while exhibits line nodes for  $0 < \kappa < 0.5$ .

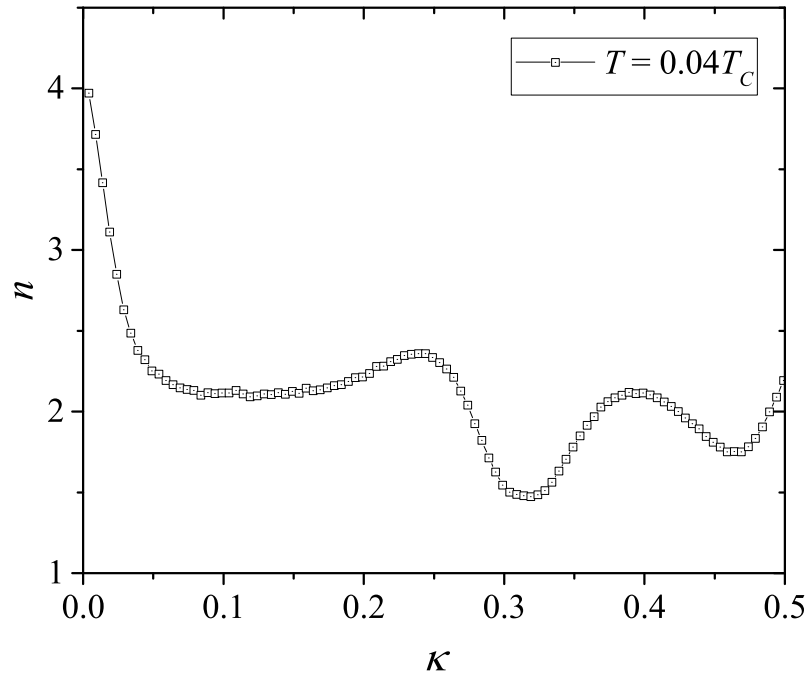


Figure 3: The exponent of temperature as a function of  $\kappa$ , calculated numerically according to  $n = d \ln(1/T_1 T) / d \ln T$ .



with increasing  $\kappa$ , and end with  $n \approx 2.2$  at  $\kappa = 0.5$ . It is worth noting that, the exponent  $n$  is not necessarily to be an integer here, similar to the cases in Ref. [23]. For  $\kappa > 0.5$ , however, the gap is open and  $1/T_1T$  decays exponentially in nature. We present in Fig. 4 the temperature dependence of  $1/T_1T$  obtained experimentally [18] by Harada *et al.* for  $Y_2C_3$ , together with the calculated results for  $\kappa=0.47, 0.50$ , and  $0.53$  for comparison. Shown in the inset of Fig. 4 is the detailed temperate dependence of  $\Delta_s$  and  $\Delta_f$  obtained by solving the gap equations Eq. (12) for  $\kappa = 0.53$ . As can be seen form Fig. 4, there is a fair agreement between our simple theory and experimental results. However, further experimental measurements at low temperatures  $T/T_c < 0.15$  are needed to obtain a decisive information about the pairing symmetry and to test the prediction of our theory.

## 5. Summary

In summary, we have calculated the temperature dependence of the nuclear magnetic relaxation rate  $1/T_1T$  in the Dresselhaus-type noncentrosymmetric superconductor  $Y_2C_3$ . We have considered the  $(s+f)$ -wave parity-mixing model where the  $d$ -vector is chosen to be parallel to the Dresselhaus SO coupling vector. It is found that various types of nodal structures can be generated due to the effect of parity-mixing, depending on the value of  $\kappa$ . We also find that, for  $\kappa \sim 0.5$ , the  $(s+f)$ -wave model can explain the experimental results fairly well over a wide range of temperatures. However, accurate measurements of  $1/T_1T$  at lower temperatures would be crucial to the further clarification of pairing symmetry and gap structure in  $Y_2C_3$ .

## 6. Acknowledgement

This work is partially supported by Science Research fund of GUCAS (No. Y25102BN00).

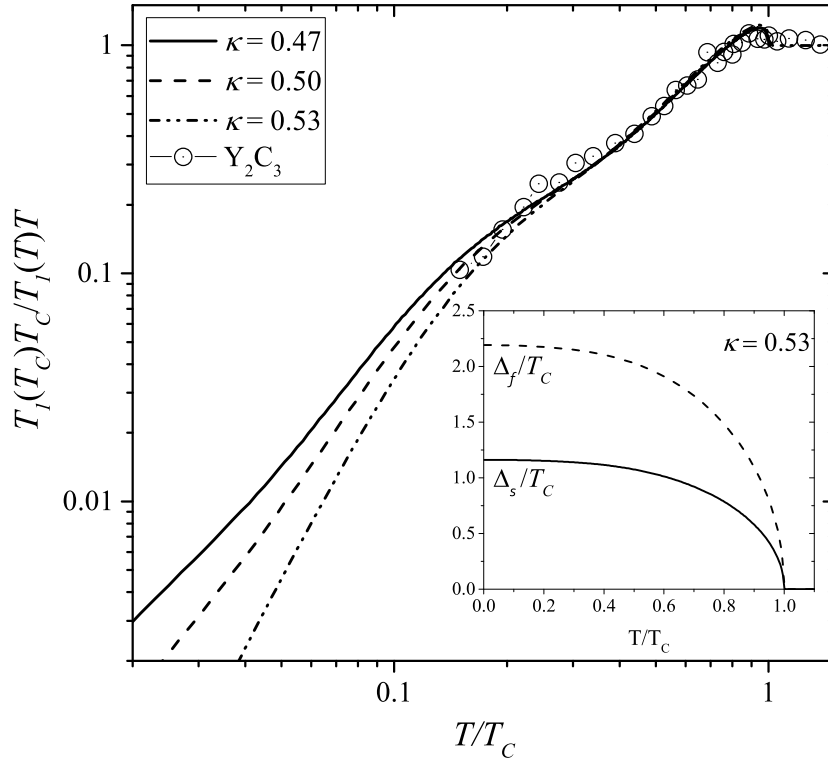


Figure 4: Comparison of the experimental data in Ref. [18] with the calculated temperature dependence of  $1/T_1T$  for  $\kappa = 0.47, 0.5, \text{ and } 0.53$ . Inset shows the temperature dependence of  $\Delta_s$  and  $\Delta_f$  at  $\kappa = 0.53$ .

## References

- [1] E. Bauer, M. Sigrist, Non-Centrosymmetric Superconductors, volume 847 of *Lecture Notes in Physics*, Springer Berlin Heidelberg, Berlin, Heidelberg, 2012. URL: <http://link.springer.com/10.1007/978-3-642-24624-1>. doi:10.1007/978-3-642-24624-1.
- [2] S. Yip, Annual Review of Condensed Matter Physics 5 (2014) 15–33. URL: <http://www.annualreviews.org/doi/abs/10.1146/annurev-conmatphys-031113-133912>. doi:10.1146/annurev-conmatphys-031113-133912.
- [3] E. Bauer, G. Hilscher, H. Michor, C. Paul, E. W. Scheidt, A. Griбанov, Y. Seropegin, H. Noël, M. Sigrist, P. Rogl, Physical Review Letters 92 (2004) 027003. URL: <http://link.aps.org/doi/10.1103/PhysRevLett.92.027003>. doi:10.1103/PhysRevLett.92.027003.
- [4] K. V. Samokhin, E. S. Zijlstra, S. K. Bose, Physical Review B 69 (2004) 094514. URL: <http://link.aps.org/doi/10.1103/PhysRevB.69.094514>. doi:10.1103/PhysRevB.69.094514.
- [5] P. W. Anderson, Physical Review B 30 (1984) 4000–4002. URL: <http://link.aps.org/doi/10.1103/PhysRevB.30.4000>. doi:10.1103/PhysRevB.30.4000.
- [6] E. I. Rashba, Sov. Phys. Solid State 2 (1960) 1109–1122.
- [7] M. Yogi, Y. Kitaoka, S. Hashimoto, T. Yasuda, R. Settai, T. D. Matsuda, Y. Haga, Y. nuki, P. Rogl, E. Bauer, Physical Review Letters 93 (2004) 027003. URL: <http://link.aps.org/doi/10.1103/PhysRevLett.93.027003>. doi:10.1103/PhysRevLett.93.027003.
- [8] K. Izawa, Y. Kasahara, Y. Matsuda, K. Behnia, T. Yasuda, R. Settai, Y. Onuki, Physical Review Letters 94 (2005) 197002.

- URL: <http://link.aps.org/doi/10.1103/PhysRevLett.94.197002>.  
doi:10.1103/PhysRevLett.94.197002.
- [9] I. Bonalde, W. Brämer-Escamilla, E. Bauer, Physical Review Letters 94 (2005) 207002. URL: <http://link.aps.org/doi/10.1103/PhysRevLett.94.207002>.  
doi:10.1103/PhysRevLett.94.207002.
- [10] A. M. Clogston, Physical Review Letters 9 (1962) 266–267. URL: <http://link.aps.org/doi/10.1103/PhysRevLett.9.266>.  
doi:10.1103/PhysRevLett.9.266.
- [11] M. Yogi, H. Mukuda, Y. Kitaoka, S. Hashimoto, T. Yasuda, R. Settai, T. D. Matsuda, Y. Haga, Y. nuki, P. Rogl, E. Bauer, Journal of the Physical Society of Japan 75 (2006) 013709. URL: <http://journals.jps.jp/doi/abs/10.1143/JPSJ.75.013709>.  
doi:10.1143/JPSJ.75.013709.
- [12] P. A. Frigeri, D. F. Agterberg, M. Sigrist, New Journal of Physics 6 (2004) 115–115. URL: <http://stacks.iop.org/1367-2630/6/i=1/a=115?key=crossref.5f0cc6a0ec027e6d4ba8390ae50516>.  
doi:10.1088/1367-2630/6/1/115.
- [13] N. Hayashi, K. Wakabayashi, P. A. Frigeri, M. Sigrist, Physical Review B 73 (2006) 092508. URL: <http://link.aps.org/doi/10.1103/PhysRevB.73.092508>.  
doi:10.1103/PhysRevB.73.092508.
- [14] G. Amano, S. Akutagawa, T. Muranaka, Y. Zenitani, J. Akimitsu, Journal of the Physical Society of Japan 73 (2004) 530–532. URL: <http://dx.doi.org/10.1143/JPSJ.73.530>. doi:10.1143/JPSJ.73.530.
- [15] G. Dresselhaus, Phys. Rev. 100 (1955) 580–586. URL: <http://link.aps.org/doi/10.1103/PhysRev.100.580>.  
doi:10.1103/PhysRev.100.580.

- [16] S. Akutagawa, J. Akimitsu, Journal of the Physical Society of Japan 76 (2007) 024713. URL: <http://journals.jps.jp/doi/abs/10.1143/JPSJ.76.024713>. doi:10.1143/JPSJ.76.024713.
- [17] T. Ekino, A. Sugimoto, A. Gabovich, H. Kinoshita, J. Akimitsu, Physica C: Superconductivity 484 (2013) 52–55. URL: <http://linkinghub.elsevier.com/retrieve/pii/S0921453412001438>. doi:10.1016/j.physc.2012.03.044.
- [18] A. Harada, S. Akutagawa, Y. Miyamichi, H. Mukuda, Y. Kitaoka, J. Akimitsu, Journal of the Physical Society of Japan 76 (2007) 023704. URL: <http://journals.jps.jp/doi/abs/10.1143/JPSJ.76.023704>. doi:10.1143/JPSJ.76.023704.
- [19] S. Kuroiwa, Y. Saura, J. Akimitsu, M. Hiraishi, M. Miyazaki, K. H. Satoh, S. Takeshita, R. Kadono, Physical Review Letters 100 (2008) 097002. URL: <http://link.aps.org/doi/10.1103/PhysRevLett.100.097002>. doi:10.1103/PhysRevLett.100.097002.
- [20] J. Chen, M. B. Salamon, S. Akutagawa, J. Akimitsu, J. Singleton, J. L. Zhang, L. Jiao, H. Q. Yuan, Physical Review B 83 (2011) 144529. URL: <http://link.aps.org/doi/10.1103/PhysRevB.83.144529>. doi:10.1103/PhysRevB.83.144529.
- [21] V. P. Mineev, K. V. Samokhin, Introduction to Unconventional Superconductivity, Gordon and Breach, London, 1999.
- [22] P. A. Frigeri, D. F. Agterberg, I. Milat, M. Sigrist, The European Physical Journal B 54 (2006) 435–448. URL: <http://www.springerlink.com/index/10.1140/epjb/e2007-00019-5>. doi:10.1140/epjb/e2007-00019-5.
- [23] B. Mazidian, J. Quintanilla, A. D. Hillier, J. F. Annett, Physical Review B 88 (2013) 224504. URL:

<http://link.aps.org/doi/10.1103/PhysRevB.88.224504>.

doi:10.1103/PhysRevB.88.224504.